Author Manuscript

Author Manuscript

Author Manuscript

Author Manuscript

HHS Public Access

Author manuscript

Environ Res. Author manuscript; available in PMC 2018 November 19.

Published in final edited form as:

Environ Res. 2018 July ; 164: 452–458. doi:10.1016/j.envres.2018.03.007.

Cerium dioxide (CeO_2) nanoparticles decrease arsenite (As(III)) cytotoxicity to 16HBE14o- human bronchial epithelial cells

Chao Zeng[1], **Chi Nguyen**[1], **Scott Boitano**[2], **Jim A. Field**[1], **Farhang Shadman**[1], and **Reyes Sierra-Alvarez**[1,*]

[1]Department of Chemical and Environmental Engineering, The University of Arizona, P.O. Box 210011, Tucson, Arizona 85704, USA

[2]Department of Physiology and The Asthma and Airway Disease Research Center, The University of Arizona, P.O. Box 210011, Tucson, Arizona 85704, USA

Abstract

The production and application of engineered nanoparticles (NPs) are increasing in demand with the rapid development of nanotechnology. However, there are concerns that some of these novel materials could lead to emerging environmental and health problems. Some NPs are able to facilitate the transport of contaminants into cells/organisms via a “Trojan Horse” effect which enhances the toxicity of the adsorbed materials. In this work, we evaluated the toxicity of arsenite (As(III)) adsorbed onto cerium dioxide (CeO_2) NPs to human bronchial epithelial cells (16HBE14o-) using the xCELLigence real time cell analyzing system (RTCA). Application of 0.5 mg/L As(III) resulted in 81.3% reduction of cell index (CI, an RTCA measure of cell toxicity) over 24 h when compared to control cells exposed to medium lacking As(III). However, when the cells were exposed to 0.5 mg/L As(III) in the presence of CeO_2 NPs (250 mg/L), the CI was only reduced by 12.9% compared to the control. The CeO_2 NPs had a high capacity for As(III) adsorption (20.2 mg/g) in the bioassay medium, effectively reducing dissolved As(III) in the aqueous solution and resulting in reduced toxicity. Transmission electron microscopy was used to study the transport of CeO_2 NPs into 16HBE14o- cells. NP uptake via engulfment was observed and the internalized NPs accumulated in vesicles. The results demonstrate that dissolved As(III) in the aqueous solution was the decisive factor controlling As(III) toxicity of 16HBE14o- cells, and that CeO_2 NPs effectively reduced available As(III) through adsorption. These data emphasize the evaluation of mixtures when assaying toxicity.

Keywords

Arsenic; Cerium dioxide; Nanomaterials; Cytotoxicity; Adsorption

1. Introduction

Nanoparticles (NPs) are defined as materials with at least one dimension between 1–100 nm in size. Their extremely small size gives NPs unique electronic, optical and chemical

*Corresponding author: P.O. Box 210011, Tucson, Arizona 85704, USA, Tel.: +1 520 621 6162; fax: +1 520 621 6048 rsierra@email.arizona.edu (R. Sierra-Alvarez).

Author Manuscript Author Manuscript Author Manuscript Author Manuscript

properties compared to their bulk counterparts (Klaine et al., 2008; Navarro et al., 2008). With the rapid development of nanotechnology, NP production and subsequent applications are growing continuously. The global production of engineered NPs is estimated to be higher than 10 million tons per year (Holden et al., 2014). The first Nanotechnology Consumer Product inventory was created in 2005, listing 54 products containing nanomaterials; in 2015, the inventory listed 1,814 products from 622 companies located in 32 countries (Vance et al., 2015). With the growing production and application of engineered NPs, environmental and unintentional human exposure is also increasing (Gottschalk and Nowack, 2011; Gottschalk et al., 2013; Keller and Lazareva, 2014; Kuhlbusch et al., 2011; Sun et al., 2014). Therefore, there are concerns that release of these novel materials may lead to emerging health problems.

So far most research has focused on the potential ecological impacts and human health effects resulted from pristine NPs (Buzea et al., 2007; Lowry et al., 2012; Nowack and Bucheli, 2007; Seaton et al., 2010), however, in the environment, NPs are present with different types of contaminants including toxic materials such as metals and metalloids. Due to the large specific surface area and surface reactivity characteristic of NPs, different contaminants could accumulate on the surface of NPs and subsequently affect the fate and toxicity of these materials. It has been reported that some NPs could act as “Trojan Horses”, enhancing the toxicity of adsorbed materials by facilitating their transport into cells or organisms. For example, lead (Pb) loaded on cerium dioxide (CeO_2) or titanium dioxide (TiO_2) NPs in the gastrointestinal tract of the water flea, *Ceriodaphnia dubia*, enhanced the bioavailability of Pb, resulting in a higher toxicity (Hu et al., 2012b). Enhanced toxic effects have been observed in experiments using arsenate (As(V)) in the presence of ferric oxide (Fe_2O_3), aluminum oxide (Al_2O_3) or TiO_2 NPs (Hu et al., 2012a; Wang et al., 2011). In a different study, nano-diamonds were shown to facilitate the transport of adsorbed heavy metals (*e.g.* Cu^{2+}) into living cells, causing subsequent release of ions in the interior of cells and leading to oxidative stress (*i.e.*, generation of reactive oxygen species (ROS)) and cytotoxicity (Zhu et al. 2015). Similarly, Limbach *et al.* (2007) observed enhanced ROS production in lung epithelial cells exposed to cobalt and manganese in the presence of nano-SiO_2 compared to the silica-free controls free of SiO_2 NPs. While information about the toxicity of NPs is valuable, it is also important to understand the synergistic effect of these materials and contaminants occurring together in the environment.

Arsenic is a well-known contaminant with high toxicity and carcinogenicity (ATSDR, 2007). Acute exposure to As can cause effects range from gastrointestinal distress to death; chronic As exposure could affect several major organ systems based on the dose (Hughes et al., 2011). The World Health Organization guideline of As in drinking water is set to 10 μg/L, while a number of large aquifers with As concentrations significantly higher than 50 μg/L have been identified in different parts of the world (Smedley and Kinniburgh, 2002). In these regions, a significant relationship between consumption of As contaminated water and increased risks of lung diseases/cancer was found (Ferreccio et al., 2000; Smith et al., 2000; Xie et al., 2014). In natural water, inorganic trivalent arsenite (As(III)) and pentavalent As(V) in the forms of oxyanions are the most predominant As species.

Author Manuscript Author Manuscript Author Manuscript Author Manuscript

Different NPs have been reported to have outstanding capacity for As(III) and As(V) adsorption (Cui et al., 2012; Feng et al., 2012; Hristovski et al., 2007; Jegadeesan et al., 2010), among them, cerium dioxide (CeO_2) is an important industrial material with the annual global production about 7,500 to 10,000 tons (Holden et al., 2014; Keller and Lazareva, 2014). CeO_2 is unique with the ease of switching the valence state (between +3 and +4 state) in favorable environment. Due to this high oxygen mobility, CeO_2 NPs are widely use in catalyst, fuel additives and medical applications (Kumar et al., 2014). In addition, a primary application of CeO_2 NPs is chemical and mechanical planarization (CMP), a key process applied to polish wafers when fabricating integrated circuits (Krishnan et al., 2010). In CMP, NPs such as CeO_2 are used in the slurry as an abrasive to remove unwanted materials on the wafer and create a flat surface. The semiconductor industry requires large amounts of water, consequently generating high volumes of wastewater. The waste stream from CMP contains high concentrations of inorganic oxide NPs and other chemicals present in the original slurry (*e.g.*, oxidizers, surfactants, dispersants, corrosion inhibitors) as well as soluble species removed from the wafer. The recent introduction of arsenic-containing materials in semiconductor manufacturing is expected to result in CMP wastewaters that also contain toxic soluble arsenic species. Arsenic containing semiconductor materials such as indium arsenide (InAs) and gallium arsenide (GaAs) are increasingly used in light emitting diodes (LEDs), liquid crystal displays (LCDs), and photovoltaics biosensors and microcircuits due to their high electron mobility, attractive optoelectric properties, and low power requirements (Dayeh, Soci, Bao, & Wang, 2009; Dick et al., 2010; Yamaguchi et al., 2008). High concentrations of dissolved arsenic species were reported in GaAs CMP wastewater (Torrance and Keenan, 2009). The potential that inorganic oxide NPs in CMP effluents (*e.g.* CeO_2) may act as carriers of toxic arsenic species is a concern. However, information about the effect of CeO_2 NPs on arsenic transport and toxicity is still lacking.

In vitro cytotoxicity assays are common alternatives to animal tests in toxicity assessment (Xing et al., 2005). Conventional cytotoxicity assays (*e.g.* MTT assay) depend on absorbance, fluorescence or luminescence measurements. These methods have a defect as the test results can be greatly obscured when measuring materials (*e.g.* mesoporous SiO_2 NPs) that tend to interfere with optical measurements (Fisichella et al., 2009; Ke et al., 2011). Also, single end-point assays provide only limited information about the interaction between testing materials and the target cells. The xCELLigence real time cell analysis (RTCA) system is a novel label-free, dynamic and high throughput technique for cytotoxicity and cell viability assessment. In this system, the biological status of adherent cells is monitored through impedance measurements (Atienza et al., 2006). Since impedance determination is not invasive, the cells remain in their normal physiological state during the assay. This system has been applied in different studies investigating the toxicity of arsenic, mercury, sodium dichromate (Xing et al., 2005) and inorganic nanoparticles(Otero-Gonzalez et al., 2012), among many other toxicants. Although RTCA measurements are reliable and highly sensitivity in cytotoxicity assessment (Limame et al., 2012), a disadvantage of this toxicity bioassay is its inability to provide mechanistic information. Nonetheless, several studies have demonstrated a strong correlation between RTCA measurements for different

Author Manuscript Author Manuscript Author Manuscript Author Manuscript

toxicants and results obtained in conventional cytotoxicity bioassays (*e.g.* MTT assay) (Otero-Gonzalez et al., 2012; Xing et al., 2005).

The objective of this study was to investigate the synergistic toxic effect of CeO_2 NPs and As(III). To this end, RTCA system was used to assess the cytotoxicity of As(III) on human bronchial epithelial cells (16HBE14o-) in the presence of CeO_2 NPs. In addition, CeO_2 uptake by 16HBE14o- cells was investigated using transmission electron microscopy (TEM). This study intends to better understand potential risks from NPs with the presence of other contaminants in the environment.

2. Materials and Methods

2.1 Materials

CeO_2 NP powder (20 nm) was obtained from MTI Corporation (Richmond, CA, USA). Minimum essential medium with Earle's salts (MEM) were purchased from Invitrogen (Carlsbad, CA, USA). Fetal bovine serum (FBS) and sodium meta-arsenite ($NaAsO_2$, ≥ 90%) were from Sigma-Aldrich (St Louis, MO, USA). In the experiments, all the solutions were prepared using ultrapure water (Milli-Q Water System, Millipore, Billerica, MA, USA).

2.2 Cell culture

In this work, 16HBE14o- cells were obtained from California Pacific Medical Center Research Institute (San Francisco, CA, USA). The cells were initially grown as described (Flynn et al., 2011). In brief, cells were grown in tissue culture flasks coated with a collagen/fibronectin/bovine serum albumin (CFB) matrix in a controlled growth medium (CGM) that contains MEM supplemented with 10% (v/v) FBS, 2 mM glutamax, penicillin and streptomycin at 37°C in a 5% CO_2 atmosphere. Subsequently, the cells were transferred to RTCA assay plates coated with CFB and maintained with a reduced serum (5% FBS) medium.

2.3 Characterization of CeO_2 NPs

The primary particle size of CeO_2 NPs was determined by transmission electron microscopy (TEM) as describe below in Section 2.8. In addition, the particle size and zeta potential (ζ potential) of the NPs (500 mg/L) in MEM were determined. The hydrodynamic particle size was measured by dynamic light scattering (DLS) using a Zetasizer Nano ZS (Malvern Instruments, Sirouthborough, MA, USA) with a laser wavelength of 633 nm and a scattering angle of 173°. ζ potential was determined by electrophoresis using the same equipment. The Smoluchowski equation was applied to correlate particle electrophoretic mobility to ζ potential value.

2.4 As(III) adsorption on CeO_2 NPs

Firstly, an As(III) stock solution (160 mg/L) was prepared, andthe pH of the solution was adjusted to near 7.0 using diluted HCl. Then the solution was diluted to 16.0, 8.0, 1.6, 0.8 and 0.16 mg/L using serum-free MEM supplemented with 2mM glutamax, penicillin and streptomycin in 50 mL centrifuge tubes with total liquid volume of 10 mL. Finally, 250

Author Manuscript Author Manuscript Author Manuscript Author Manuscript

mg/L CeO_2 NPs were added into each tube. The dispersions were mixed for 48 h using an orbital shaker at 150 rpm at room temperature (25 °C) to attain adsorption equilibrium. NP-free As(III) solutions were run in parallel during this process. After 48 h, the suspensions/solutions were collected for analysis of dissolved As(III). The samples were first centrifuged at 13,300 g for 10 min, and then the supernatants were filtered through 25-nm membrane filters to remove all the particles. The concentration of As in the filtrates was determined by inductively coupled plasma-optical emission spectroscopy (ICP-OES, 5100, Agilent Technologies, Santa Clara, CA, USA) at a wavelength of 188.98 nm. The amount of As(III) adsorbed on CeO_2 NPs was calculated from mass balance.

In this study, Langmuir and Freundlich isotherms were applied to describe As(III) adsorption onto CeO_2 NPs. The equation of Langmuir isotherm is shown as follows:

$$\frac{C_e}{q_e} = \frac{1}{K_{eq} \cdot q_{max}} + \frac{C_e}{q_{max}} \quad (1)$$

where C_e [mg/L] is the equilibrium concentration, q_e [mg/g] is the amount of As(III) adsorbed on the solid, K_{eq} [L/mg] is the adsorption equilibrium constant and q_{max} [mg/g] is the adsorption capacity. The Freundlich isotherm is expressed as follows:

$$q_e = K_f C_e^{1/n} \quad (2)$$

where K_f [(mg/g)/(mg/L)$^{1/n}$] and n (dimensionless) are the Freundlich constants. The adsorption parameters were acquired by fitting the experimental data into those two models using the software OriginPro 9.1 (OriginLab Corp., Northampton, MA, USA).

2.5 RTCA assay

The xCELLigence RTCA instrument (ACEA Biosciences, San Diego, CA, USA) is a novel system allows for dynamic monitoring cytotoxicity and cell proliferation based on impedance measurements. The instrument is placed in a standard CO_2 cell culture incubator and interfaces via a cable with analysis and control units that are housed outside the incubator (www.aceabio.com). Assays are conducted in 96-well E-plates with plate cover (E-Plate 96; ACEA Biosciences; plate dimensions: 12.77 cm x 8.55 cm x 1.75 cm (W x D x H)). The volume of each well is 243 μL ± 5 μL, and the well diameter is 5.0 mm ± 0.05 mm. When cells attach to the plate, they create impedance that can be detected by the interdigitated gold microelectrodes integrated on the bottom of the testing plate. Measured impedance is calculated and plotted as cell index (CI), which is proportional to cell biological statuses as cell number, morphology and adhesion. The principles of RT-CES technology have been described previously (Atienza et al., 2006; Xing et al., 2005).

As shown in Fig. 1, the background impedance (or baseline) is measured with only assay medium. CI value increases after the introduction of the cells, and the number becomes higher with increased cell number, size and spreading until it reaches the plateau when the

Author Manuscript Author Manuscript Author Manuscript Author Manuscript

well is 100% covered. The introduction of cytotoxicity inducing agents leads to cell detachment or cell death, which results in a decreased CI (or negative slope) as show in Fig. 1 (red line). Some materials are not able to cause cell death but can inhibit cell viability/proliferation, in this case, it creates a curve with positive slope but with CI values lower than the control.

2.6 As(III) toxicity to 16HBE14o- cells in the presence of CeO_2 NPs

As(III) solutions (2, 10 and 20 mg/L) were first prepared in 10 mL MEM in 50 mL centrifuge tubes (pH adjusted to about 7.0). CeO_2 NPs (1 g/L) were then added into each vial. The mixtures were mixed for 48 h under the same conditions as described in *Section 2.4*. In this step, NP-free As(III) solutions and CeO_2 dispersions (1 g/L) were run in parallel. The concentrations of dissolved As(III) were measured as described in *Section 2.4*. After this pre-adsorption step, the cytotoxicity of As(III) in the presence and absence of CeO_2 NPs was evaluated using the RTCA assay.

In the RTCA assay, 16HBE14o- cells were first plated onto 96-well E-plates (ACEA Biosciences, San Diego, CA, USA) at a cell density of ~100,000 cells/well (150 μL). Then the cells were incubated at 37°C and 5% CO_2 to verify proper growth. During this growth period, the impedance was continuously monitored using an xCELLigence MP instrument. After about 20 h, 50 μL of As(III) stock solutions (in the presence/absence of CeO_2 NPs) were added to each well. The final volume of the solution in each well was 200 μL and the final concentrations of the testing materials were one quarter as compared to the stock. CI values were measured and recorded every 15 min for 48 h. In the experiments, assays were performed in quadruplicate and appropriate controls (e.g., controls without As(III) and NPs, and controls without As(III) but lacking NPs) were run in parallel.

The normalized cell index (NCI) was calculated for data analysis using the following equation:

$$NCI_t = \frac{CI_t}{CI_0} \quad (3)$$

where CI_t is the CI at any time t and CI_0 is the CI at the time of toxicant dosing (where NCI is equal to 1). The percent inhibition was then calculated based on NCI values using the following equations:

$$Inhibition(\%) = \frac{NCI(control) - NCI(sample)}{NCI(control) - 1} \times 100 \quad (4)$$

when the NCI values of the samples were less than 1, inhibition values were reported as 100%. The inhibition was calculated based on the NCI values determined in controls lacking As(III) and NPs.

Author Manuscript Author Manuscript Author Manuscript Author Manuscript

2.7 Uptake of CeO_2 NPs by 16HBE14o- cells

Approximately 550,000 cells in MEM supplemented with 5% FBS, 2 mM glutamax and pen/strep were plated onto 6-well plates coated with CFB and incubated for 24 h. The cells were then exposed to 250 mg/L CeO_2 NPs for 24 h. Finally, the cells were prepared for TEM measurements after washing by Hank's balanced salt solution (HBSS).

2.8 Transmission electron microscopy

The primary particle size of CeO_2 NPs was determined by TEM using a Tecnai G2 Spirit Biotwin instrument operated at 100 kV as described (Ramos-Ruiz et al., 2016). Washed cells exposed to nanoparticles were pre-fixed with 2.5% glutaraldehyde overnight and then fixed with 1% osmium in 0.1M PIPES at pH 7.4 for 30 min. After fixation, the cells were washed twice with demineralized water (DI) for 5 min, and centrifuged at 3200 rpm for 10 min. The cells were stained with 2% aqueous uranyl acetate for 20 min, washed with DI water for 5 min, and then dehydrated by immersion in aqueous solutions containing increasing ethanol concentration (50, 70, 90 and 100% each for 5 min, followed by washing with 100% ethanol for 20 min). Finally, the cell pellet was embedded in resin Embed 812 (resin/acetonitrile (1:1) overnight, followed by incubation in resin at room temperature for 60 min (three times), and polymerization at 60°C for 24 h). Ultra-thin slices (70–100 nm) of embedded cells were obtained using a microtome (Leica EM UC7m Buffalo Grove, IL, USA) and collected on 200 mesh grids. Sections were examined with a Tecnai G2 TEM (FEI Company, Hillsboro, OR, USA) operated at a power intensity of 100 kV.

2.9 Statistical analysis

The statistical analysis was performed using a two-sample t-test assuming unequal variances on Microsoft Excel. The statistical comparison was based upon the t-critical two-tail values and the t-stat values. Significance was considered to be at the $p < 0.05$ probability level.

3. Results and discussion

3.1 Characterization of CeO_2 NPs

Fig. 2 shows a TEM image of the CeO_2 NPs. The figure shows that some of NPs have a sphere-like shape with a diameter of about 8 nm; while others have a rod-like shape with a length of about 35 nm and a diameter of about 10 nm. The hydrodynamic diameter of the NPs was 1463.0 ± 108.9 nm. DLS data showed that the polydispersity index (PDI) of particle dispersion was 0.29. The ζ potential of CeO_2 was −7.2 ± 1.1 mV. These results indicated particle aggregation in MEM. Colloidal dispersions with ζ potential values higher than +30 mV or lower than −30 mV are considered stable (Howe et al., 2012), while particles with low surface charge tend to aggregate due to limited electrostatic repulsion forces. The pH of the MEM solution is around 7.0, within the reported point zero charge (PZC) range of CeO_2 NPs (6.7–8.6) (Cornelis et al., 2011; Oriekhova and Stoll, 2016; Otero-Gonzalez et al., 2014). This can explain the low particle surface charge observed in the experiment. In addition, MEM contains high concentrations of $NaHCO_3$ (2.2 g/L), NaCl (6.8 g/L) and other salts. The high ionic strength can compress the electrical double layer and, consequently, lower the energy barrier promoting particle agglomeration.

Author Manuscript Author Manuscript Author Manuscript Author Manuscript

3.2 As(III) adsorption on CeO_2 NPs

Fig. 3 shows the adsorption equilibrium isotherms of As(III) on CeO_2 NPs in MEM. The experimental data were fitted with Freundlich and Langmuir models described in *Section 2.4*, the parameters obtained from the fitting are summarized in Table 1. The results show that although As(III) adsorption by the CeO_2 NPs can be described well by both models, the Langmuir isotherm provided slightly better fitting. Different from Freundlich adsorption isotherm that is an empirical model, Langmuir isotherm assumes monolayer adsorption and no interaction between adsorption sites (Dutta et al., 2004). The adsorption capacity (q_{max}) acquired form the model was 20.2 mg As(III)/g CeO_2. So far there is only one study that has investigated the adsorption characteristics of As(III) on CeO_2 NPs in water, in which the reported q_{max} is 18.0 mg As(III)/g CeO_2 (Feng et al., 2012). Some other widely used NPs have also been studied for their potential on As(III) removal. For example, the q_{max} values for nanoscale zero-valent iron and Fe_2O_3 at neutral pH are 1.8 and 2.5 mg As(III)/g sorbent, respectively (Kanel et al., 2005; Prasad et al., 2011). When using high initial As(III) concentrations (up to 80 mg/L), the q_{max} was reported in the range of 46.1–57.5 mg/g for nanocrystalline titanium dioxide (TiO_2) (Pena et al., 2005). In summary, CeO_2 NPs showed comparatively high efficiency for As(III) adsorption, which may pose an impact on the fate, transport and toxicity of aqueous As(III).

3.3 As(III) toxicity to 16HBE14o- cells with the presence of CeO_2 NPs

This study investigated the response of 16HBE14o- cells to different concentrations of As(III) in the presence and absence of CeO_2 NPs (Fig. 4). Human epithelial cells represent a primary target tissue from environmental toxicants (Feng et al., 2015). These cells are also important as they form a barrier to the environment and protect more sensitive underlying tissue of various organs. 16HBE14o-, an adherent and immortalized human bronchial epithelial cell line, is often used as a model cell type to study pulmonary adsorption, transport and permeability to airway exposure (Ehrhardt et al., 2003; Forbes et al., 2003; Sherwood et al., 2013).

Cells exposed to As(III) showed a characteristic pattern distinguished by an initial transient NCI increase in values during the first 5 h after As(III) dosing, thereafter the NCIs decreased dropping below the NCIs of the control culture lacking As(III). In addition, the characteristic response was dose-dependent as the higher the level of As(III) led to a more significant initial NCI increase and subsequent NCI decrease. The RTCA system has been reported to generate agent-specific kinetic profiles (Limame et al., 2012). This technique has been applied in a previous study investigating the effect of As(III) on NIH 3T3 cells (Kanel et al., 2005), in which the characteristic cell response pattern was also observed at the dose range from 1.3 to 29.6 μM (about 0.1 to 2.2 mg/L As).

In the current study, As(III) was highly inhibitory to 16HBE14o- cells as evidenced by NCI values of the samples exposed to As(III) solutions were much lower than those from the control after 48 h. As(III) caused marked cytotoxicity leading to cell death at concentrations of 5.0 mg/L (Fig. 4A) and 2.5 mg/L (Fig. 4B). The NCIs of these samples decreased continuously after the initial transient increase and became lower than 1.0 after 15 and 40 h of exposure, respectively. Especially for the samples exposed to 5.0 mg/L of As(III), most of

Author Manuscript Author Manuscript Author Manuscript Author Manuscript

the cells were detached from the plate after 48 h. At 0.5 mg/L, As(III) did not lead to considerable cell death, however, it caused significant reduction on cell viability and proliferation as the NCI was only slightly higher than the initial value but much lower than that of the control after 48 h of exposure. As(III) toxic effects on human bronchial epithelial cells have been reported in different studies. For example, a study found that exposure to 0.75 mg/L of As(III) reduced the relative cell survival to 59% after 24 h exposure in a clonogenic assay (a cell survival assay assessing the effects of an agent on cell proliferation) (Xie et al., 2014). In another study, exposure to the same concentration of As(III) led to 80% inhibition in MTT conversion (MTT assay is a widely used physiological end-point assay that evaluates cell viability) (Styblo et al., 2000). In both studies, normal human bronchial epithelial cells were used. Despite the differences between the assays, our results are generally in agreement with these previous studies indicating that As(III) can cause acute toxic effects to human lung cells even at relatively low concentrations. The toxicity of As(III) has been attributed to oxidative stress due to the generation of reactive oxygen species (Li et al., 2014). As(III) has also been shown to alter cell signaling and compromise wound response of 16HBE14o- cells (Sherwood et al., 2011).

In this work, CeO_2 NPs (250 mg/L) were not toxic to the cells as the NCI values from the sample exposed to CeO_2 NP alone were very close to those from the control cells lacking CeO_2 NP. In addition, CeO_2 NPs decreased the toxic effects exerted by As(III) as the NCIs of the treatments with As(III) and CeO_2 NPs were much higher than those exposed to As(III) alone after 48 h of exposure. As shown in Fig. 4A, the presence of CeO_2 NPs lowered the rate of cell death for cells exposed to 5.0 mg/L As(III) (less steep negative slope). Exposure to 2.5 mg/L As(III) led to significant cell death, however, in the presence of CeO_2 NPs no clear cell death was observed and the treatment only inhibited cell viability and proliferation (Fig. 4B). The reduction in As(III)-mediated toxicity was most significant for the samples containing 0.5 mg/L of As(III) together with CeO_2 NPs. In those assays, the inhibition caused by As(III) after 48 h of incubation was 81.3% compared to only 12.9% when the cells were exposed to the same concentration of As(III) in the presence of CeO_2 NPs (Fig. 4C). A detailed comparison of the percent inhibition data is summarized in Fig. S1 (Supplementary Information).

Table 2 shows the concentrations of dissolved As(III) in the MEM medium after the pre-adsorption step as described *Section 2.6*. It is clear that the adsorption of As(III) onto CeO_2 NPs significantly decreased the concentrations of soluble As(III) remaining in the aqueous solution. The correlation between NCI values at 48 h and dissolved As(III) concentrations was summarized in Fig. S2 (Supplementary Information). This result indicates that the decreased toxicity observed in the experiment was due to the reduced As(III) concentration in the aqueous solution. In order to better understand the mechanism of this detoxification effect, CeO_2 NP uptake by 16HBE14o- cells was investigated.

3.4 CeO_2 NP uptake by 16HBE14o- cells

In this work, internalization of CeO_2 NPs by human bronchial epithelial cells was observed. As shown in Fig. 5, the NPs were taken up and they accumulated in cell vesicles. Although the nature of the vesicles could not ascertain based on the TEM images, for the sake of this

Author Manuscript Author Manuscript Author Manuscript Author Manuscript

discuss we hypothesize that the observed vesicles were most likely lysosomes. Lysosomes are vesicles found in cells that function as “garbage disposal”, involved in the degradation of biomolecules and xenobiotic materials originating outside the cell. Previous studies have shown that NP uptake through endocytic routes often converge in the lysosome and that lysosomes are is the most common intracellular site for NP sequestration and degradation (Stern et al., 2012). A variety of widely used NPs (such as TiO_2, silver and SiO_2) have been reported to cause lysosomal dysfunction, and subsequently lead to adverse effects on cells including cell death (Stern et al., 2012). Although numerous studies have been conducted to investigate the cytotoxicity of CeO_2 NPs, cytotoxic effects resulting from lysosomal NP accumulation has not been reported (Song et al., 2014; Stern et al., 2012; Strobel et al., 2015). In this work CeO_2 NP uptake by human bronchial epithelial cells was observed. However, the uptake did not lead to any acute toxicity as described in *Section 3.3*.

Hydrolytic enzymes and acidic pH (4.5–5.0) occur in the lysosome creating an environment that facilitates the degradation of unwanted biopolymers in the cells (Mindell, 2012). The acidic environment in lysosome could also trigger the release of toxic ions and increase toxicity. Sabella and coworkers have coined the term “lysosome-enhanced Trojan Horse effect” to describe that effect (Sabella et al., 2014). In this work, opposite results were observed. Uptake and accumulation of As(III)-loaded CeO_2 NPs in cell vesicles did not enhance the toxicity of As(III). Although lysosomes have an acidic pH, this does not necessarily lead to significant As(III) desorption from CeO_2 NPs. Firstly, CeO_2 NPs are insoluble at the pH in the lysosome (Dahle et al., 2015), therefore, there should be no As(III) release due to CeO_2 dissolution. Secondly, the acidic environment in the lysosome only has a limited effect on the affinity of CeO_2 NPs for As(III). Feng and coworkers have reported that the adsorption of As(III) on CeO_2 NPs only decreased about 10% at mild acidic pH (pH 4–6) compared to the data measured at neutral pH range (Feng et al., 2012). In the same study, desorption hysteresis (referred as irreversible adsorption) was reported. After adsorption equilibrium, desorption experiment showed that the released As accounted only for a portion (maximum 40%) of total As adsorbed. Overall, the results show that the dissolved As(III) in the aqueous solution had much higher bioavailability than the As absorbed onto CeO_2 NPs.

4. Conclusions

As(III) in solution is highly inhibitory to human bronchial epithelial cells. As(III) adsorbed onto CeO_2 NPs diminishes the inhibitory impact of As(III) by lowering its aqueous concentration. As(III) loaded CeO_2 NPs taken up by cells accumulated in the lysosomes, but the acidic environment of lysosomes did not lead to massive As(III) release.

Supplementary Material

Refer to Web version on PubMed Central for supplementary material.

Author Manuscript Author Manuscript Author Manuscript Author Manuscript

Acknowledgements

This work was supported by the Semiconductor Research Corporation (SRC) Engineering Research Center for Environmental Benign Semiconductor Manufacturing (Award # 425.052), by the National Science Foundation (NSF-CBET/GOALI Award #1507446) and by the National Institutes of Health (ES 04940).

References

Atienza JM, Yu NC, Kirstein SL, Xi B, Wang XB, Xu X, Abassi YA, 2006 Dynamic and label-free cell-based assays using the real-time cell electronic sensing system. Assay Drug Dev Techn 4, 597–607.

ATSDR, 2007 Toxicological Profile for Arsenic, in: Agency for Toxic Substances and Disease Registry, U.S. Department of Health and human Service (Ed.), Atlanta, GA.

Buzea C, Pacheco II, Robbie K, 2007 Nanomaterials and nanoparticles: Sources and toxicity. Biointerphases 2, Mr17–Mr71. [PubMed: 20419892]

Cornelis G, Ryan B, McLaughlin MJ, Kirby JK, Beak D, Chittleborough D, 2011 Solubility and batch retention of CeO_2 nanoparticles in soils. Environ Sci Technol 45, 2777–2782. [PubMed: 21405081]

Cui H, Li Q, Gao SA, Shang JK, 2012 Strong adsorption of arsenic species by amorphous zirconium oxide nanoparticles. J Ind Eng Chem 18, 1418–1427.

Dahle JT, Livi K, Arai Y, 2015 Effects of pH and phosphate on CeO_2 nanoparticle dissolution. Chemosphere 119, 1365–1371. [PubMed: 24630459]

Dayeh SA, Soci C, Bao X-Y, Wang D, 2009 Advances in the synthesis of InAs and GaAs nanowires for electronic applications. Nano Today, 4(4), 347–358.

Dick KA, Caroff P, Bolinsson J, Messing ME, Johansson J, Deppert K, Wallenberg LR, Samuelson L, 2010 Control of III-V nanowire crystal structure by growth parameter tuning. Semicond Sci Tech 25(2).

Dutta PK, Ray AK, Sharma VK, Millero FJ, 2004 Adsorption of arsenate and arsenite on titanium dioxide suspensions. J Colloid Interf Sci 278, 270–275.

Ehrhardt C, Kneuer C, Laue M, Schaefer UF, Kim KJ, Lehr CM, 2003 16HBE14o- human bronchial epithelial cell layers express P-glycoprotein, lung resistance-related protein, and caveolin-1. Pharmaceut Res 20, 545–551.

Feng QZ, Zhang ZY, Ma YH, He X, Zhao YL, Chai ZF, 2012 Adsorption and desorption characteristics of arsenic onto ceria nanoparticles. Nanoscale Res Lett 7, 1–8. [PubMed: 22214494]

Feng WQ, Guo JJ, Huang HY, Xia B, Liu HY, Li J, Lin SL, Li TY, Liu JJ, Li H, 2015 Human normal bronchial epithelial cells: A novel in vitro cell model for toxicity evaluation. Plos One 10.

Ferreccio C, Gonzalez C, Milosavjlevic V, Marshall G, Sancha AM, Smith AH, 2000 Lung cancer and arsenic concentrations in drinking water in Chile. Epidemiology 11, 673–679. [PubMed: 11055628]

Fisichella M, Dabboue H, Bhattacharyya S, Saboungi ML, Salvetat JP, Hevor T, Guerin M, 2009 Mesoporous silica nanoparticles enhance MTT formazan exocytosis in HeLa cells and astrocytes. Toxicol in Vitro 23, 697–703. [PubMed: 19254755]

Flynn AN, Tillu DV, Asiedu MN, Hoffman J, Vagner J, Price TJ, Boitano S, 2011 The Protease-activated Receptor-2-specific Agonists 2-aminothiazol-4-yl-LIGRL-NH2 and 6-aminonicotinyl-LIGRL-NH2 stimulate multiple signaling pathways to induce physiological responses in vitro and in vivo. J Biol Chem 286, 19076–19088. [PubMed: 21467041]

Forbes B, Shah A, Martin GP, Lansley AB, 2003 The human bronchial epithelial cell line 16HBE14o- as a model system of the airways for studying drug transport. Int J Pharm 257, 161–167. [PubMed: 12711171]

Gottschalk F, Nowack B, 2011 The release of engineered nanomaterials to the environment. J Environ Monitor 13, 1145–1155.

Gottschalk F, Sun TY, Nowack B, 2013 Environmental concentrations of engineered nanomaterials: Review of modeling and analytical studies. Environ Pollut 181, 287–300. [PubMed: 23856352]

Author Manuscript Author Manuscript Author Manuscript Author Manuscript

Howe KJ, Hand DW, Crittenden JC, Trussell RR, Tchobanoglous G, 2012 Principles of Water Treatment. Wiley.

Holden PA, Klaessig F, Turco RF, Priester JH, Rico CM, Avila-Arias H, Mortimer M, Pacpaco K, Gardea-Torresdey JL, 2014 Evaluation of exposure concentrations used in assessing manufactured nanomaterial environmental hazards: Are they relevant? Environ Sci Technol 48, 10541–10551. [PubMed: 25158225]

Hristovski K, Baumgardner A, Westerhoff P, 2007 Selecting metal oxide nanomaterials for arsenic removal in fixed bed columns: From nanopowders to aggregated nanoparticle media. J Hazard Mater 147, 265–274. [PubMed: 17254707]

Hu J, Wang DM, Forthaus BE, Wang JM, 2012a Quantifying the effect of nanoparticles on As(V) ecotoxicity exemplified by nano-Fe2O3 (magnetic) and nano-Al2O3. Environ Toxicol Chem 31, 2870–2876. [PubMed: 22997023]

Hu J, Wang DM, Wang JT, Wang JM, 2012b Toxicity of lead on *Ceriodaphnia dubia* in the presence of nano-CeO_2 and nano-TiO_2. Chemosphere 89, 536–541. [PubMed: 22682362]

Hughes MF, Beck BD, Chen Y, Lewis AS, Thomas DJ, 2011 Arsenic exposure and toxicology: A historical perspective. Toxicol Sci 123, 305–332. [PubMed: 21750349]

Jegadeesan G, Al-Abed SR, Sundaram V, Choi H, Scheckel KG, Dionysiou DD, 2010 Arsenic sorption on TiO_2 nanoparticles: Size and crystallinity effects. Water Res 44, 965–973. [PubMed: 20022353]

Kanel SR, Manning B, Charlet L, Choi H, 2005 Removal of arsenic(III) from groundwater by nanoscale zero-valent iron. Environ Sci Technol 39, 1291–1298. [PubMed: 15787369]

Ke N, Wang XB, Xu X, Abassi YA, 2011 The xCELLigence system for real-time and label-free monitoring of cell viability. Methods Mol Biol 740, 33–43. [PubMed: 21468966]

Keller AA, Lazareva A, 2014 Predicted releases of engineered nanomaterials: From global to regional to local. Environ Sci Tech Let 1, 65–70.

Klaine SJ, Alvarez PJJ, Batley GE, Fernandes TF, Handy RD, Lyon DY, Mahendra S, McLaughlin MJ, Lead JR, 2008 Nanomaterials in the environment: Behavior, fate, bioavailability, and effects. Environ Toxicol Chem 27, 1825–1851. [PubMed: 19086204]

Krishnan M, Nalaskowski JW, Cook LM, 2010 Chemical mechanical planarization: Slurry chemistry, materials, and mechanisms. Chem Rev 110, 178–204. [PubMed: 19928828]

Kuhlbusch TAJ, Asbach C, Fissan H, Gohler D, Stintz M, 2011 Nanoparticle exposure at nanotechnology workplaces: A review. Part Fibre Toxicol 8.

Kumar A, Das S, Munusamy P, Self W, Baer DR, Sayle DC, Seal S 2014 Behavior of nanoceria in biologically-relevant environments. Environ Sci: Nano 1(6), 516–532.

Li LZ, Qiu P, Chen BL, Lu YJ, Wu K, Thakur C, Chang QS, Sun JY, Chen F, 2014 Reactive oxygen species contribute to arsenic-induced EZH2 phosphorylation in human bronchial epithelial cells and lung cancer cells. Toxicol Appl Pharm 276, 165–170.

Limame R, Wouters A, Pauwels B, Fransen E, Peeters M, Lardon F, De Wever O, Pauwels P, 2012 Comparative analysis of dynamic cell viability, migration and invasion assessments by novel real-time technology and classic endpoint assays. Plos One 7.

Limbach LK, Wick P, Manser P, Grass RN, Bruinink A, Stark WJ, 2007 Exposure of engineered nanoparticles to human lung epithelial cells: Influence of chemical composition and catalytic activity on oxidative stress. Environ Sci Technol 41, 4158–4163. [PubMed: 17612205]

Lowry GV, Gregory KB, Apte SC, Lead JR, 2012 Transformations of nanomaterials in the environment. Environ Sci Technol 46, 6893–6899. [PubMed: 22582927]

Mindell JA, 2012 Lysosomal acidification mechanisms. Annu Rev Physiol 74, 69–86. [PubMed: 22335796]

Navarro E, Baun A, Behra R, Hartmann NB, Filser J, Miao AJ, Quigg A, Santschi PH, Sigg L, 2008 Environmental behavior and ecotoxicity of engineered nanoparticles to algae, plants, and fungi. Ecotoxicology 17, 372–386. [PubMed: 18461442]

Nowack B, Bucheli TD, 2007 Occurrence, behavior and effects of nanoparticles in the environment. Environ Pollut 150, 5–22. [PubMed: 17658673]

Oriekhova O, Stoll S, 2016 Effects of pH and fulvic acids concentration on the stability of fulvic acids - cerium (IV) oxide nanoparticle complexes. Chemosphere 144, 131–137. [PubMed: 26347935]

Author Manuscript Author Manuscript Author Manuscript Author Manuscript

Otero-Gonzalez L, Barbero I, Field JA, Shadman F, Sierra-Alvarez R, 2014 Stability of alumina, ceria, and silica nanoparticles in municipal wastewater. Water Sci Technol 70, 1533–1539. [PubMed: 25401318]

Otero-Gonzalez L, Sierra-Alvarez R, Boitano S, Field JA, 2012 Application and validation of an impedance-based real time cell analyzer to measure the toxicity of nanoparticles impacting human bronchial epithelial cells. Environ Sci Technol 46, 10271–10278. [PubMed: 22916708]

Pena ME, Korfiatis GP, Patel M, Lippincott L, Meng XG, 2005 Adsorption of As(V) and As(III) by nanocrystalline titanium dioxide. Water Res 39, 2327–2337. [PubMed: 15896821]

Prasad B, Ghosh C, Chakraborty A, Bandyopadhyay N, Ray RK, 2011 Adsorption of arsenite (As3+) on nano-sized Fe2O3 waste powder from the steel industry. Desalination 274, 105–112.

Ramos-Ruiz A, Field JA, Wilkening JV, Sierra-Alvarez R, 2016 Recovery of elemental tellurium nanoparticles by the reduction of tellurium oxyanions in a methanogenic microbial consortium. Environ Sci Technol 50, 1492–1500. [PubMed: 26735010]

Sabella S, Carney RP, Brunetti V, Malvindi MA, Al-Juffali N, Vecchio G, Janes SM, Bakr OM, Cingolani R, Stellacci F, Pompa PP, 2014 A general mechanism for intracellular toxicity of metal-containing nanoparticles. Nanoscale 6, 7052–7061. [PubMed: 24842463]

Seaton A, Tran L, Aitken R, Donaldson K, 2010 Nanoparticles, human health hazard and regulation. J R Soc Interface 7, S119–S129. [PubMed: 19726441]

Sherwood CL, Lantz RC, Boitano S, 2013 Chronic arsenic exposure in nanomolar concentrations compromises wound response and intercellular signaling in airway epithelial cells. Toxicol Sci 132, 222–234. [PubMed: 23204110]

Sherwood CL, Lantz RC, Burgess JL, Boitano S, 2011 Arsenic alters ATP-dependent Ca^{2+} signaling in human airway epithelial cell wound response. Toxicol Sci 121, 191–206. [PubMed: 21357385]

Smedley PL, Kinniburgh DG, 2002 A review of the source, behaviour and distribution of arsenic in natural waters. Appl Geochem 17, 517–568.

Smith AH, Lingas EO, Rahman M, 2000 Contamination of drinking-water by arsenic in Bangladesh: a public health emergency. B World Health Organ 78, 1093–1103.

Song WS, Lee SS, Savini M, Popp L, Colvin VL, Segatori L, 2014 Ceria nanoparticles stabilized by organic surface coatings activate the lysosome-autophagy system and enhance autophagic clearance. ACS Nano 8, 10328–10342. [PubMed: 25315655]

Stern ST, Adiseshaiah PP, Crist RM, 2012 Autophagy and lysosomal dysfunction as emerging mechanisms of nanomaterial toxicity. Part Fibre Toxicol 9.

Strobel C, Oehring H, Herrmann R, Forster M, Reller A, Hilger I, 2015 Fate of cerium dioxide nanoparticles in endothelial cells: exocytosis. J Nanopart Res 17.

Styblo M, Del Razo LM, Vega L, Germolec DR, LeCluyse EL, Hamilton GA, Reed W, Wang C, Cullen WR, Thomas DJ, 2000 Comparative toxicity of trivalent and pentavalent inorganic and methylated arsenicals in rat and human cells. Arch Toxicol 74, 289–299. [PubMed: 11005674]

Sun TY, Gottschalk F, Hungerbuhler K, Nowack B, 2014 Comprehensive probabilistic modelling of environmental emissions of engineered nanomaterials. Environ Pollut 185, 69–76. [PubMed: 24220022]

Vance ME, Kuiken T, Vejerano EP, McGinnis SP, Hochella MF, Rejeski D, Hull MS, 2015 Nanotechnology in the real world: Redeveloping the nanomaterial consumer products inventory. Beilstein J Nanotech 6, 1769–1780.

Wang DM, Hu J, Irons DR, Wang JM, 2011 Synergistic toxic effect of nano-TiO2 and As(V) on Ceriodaphnia dubia. Sci Total Environ 409, 1351–1356. [PubMed: 21239047]

Xie H, Huang SP, Martin S, Wise JP, 2014 Arsenic is cytotoxic and genotoxic to primary human lung cells. Mutat Res-Gen Tox En 760, 33–41.

Xing JZ, Zhu LJ, Jackson JA, Gabos S, Sun XJ, Wang XB, Xu X, 2005 Dynamic monitoring of cytotoxicity on microelectronic sensors. Chem Res Toxicol 18, 154–161. [PubMed: 15720119]

Yamaguchi M, Nishimura KI, Sasaki T, Suzuki H, Arafune K, Kojima N, Ohsita Y, Okada Y, Yamamoto A, Takamoto T, Araki K, 2008 Novel materials for high-efficiency III-V multi-junction solar cells. Sol Energy, 82(2), 173–180.

Author Manuscript Author Manuscript Author Manuscript Author Manuscript

Zhu Y, Zhang Y, Shi GS, Yang JR, Zhang JC, Li WX, Li AG, Tai RZ, Fang HP Fan CH, Huang Q, 2015 Nanodiamonds act as Trojan horse for intracellular delivery of metal ions to trigger cytotoxicity, Part Fibre Toxicol 12.

Author Manuscript Author Manuscript Author Manuscript Author Manuscript

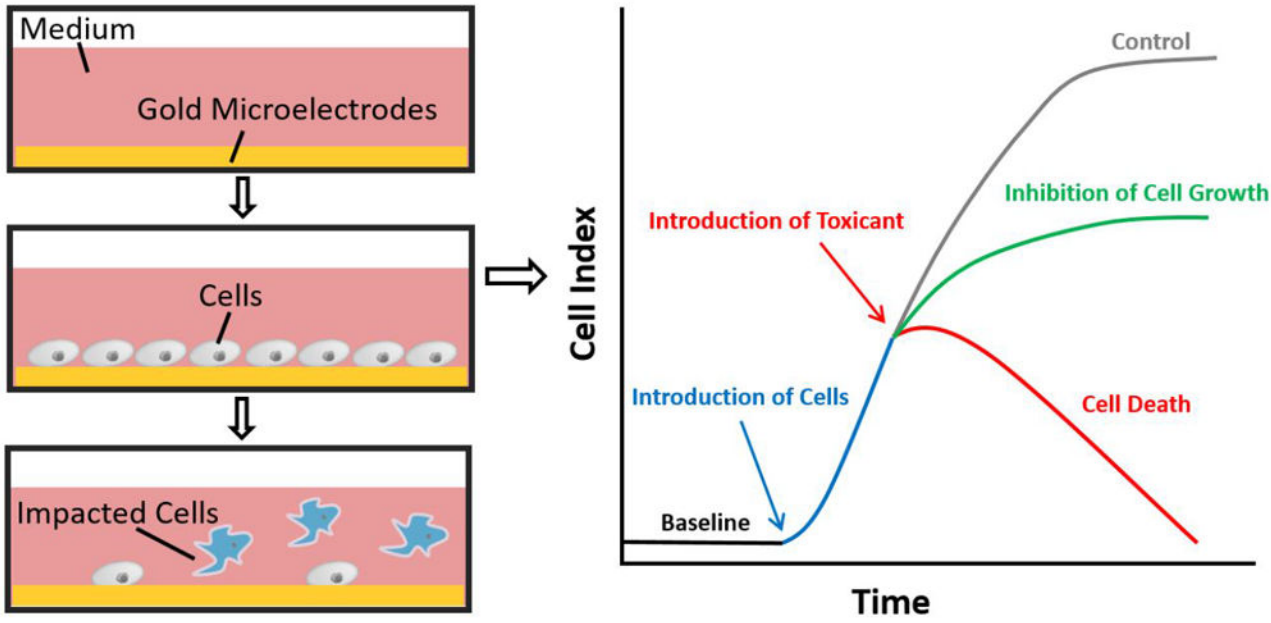

Fig. 1.

Impedance-based real time cell analysis system. Impedance changes due to cell adherence are detected by the interdigitated gold microelectrodes on the well bottom of the testing plate. The detection is proportional to cell biological status as cell number, morphology and adhesion. Increased cell number and spreading results in a higher value. In this system, the measured impedance is expressed as Cell Index (CI). The CI is defined as $(R_n\text{-}R_b)/15$, where R_n is the impedance of the well when it contains cells and R_b is the background impedance measured with only the medium.

Author Manuscript Author Manuscript Author Manuscript Author Manuscript

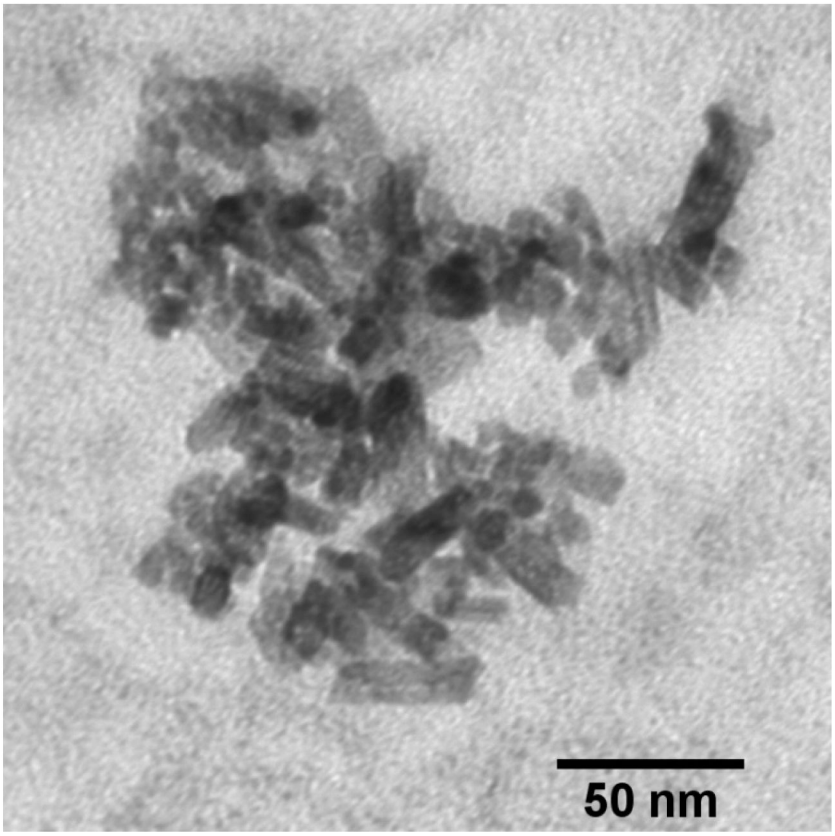

Fig. 2.
TEM image of CeO_2 NPs.

Author Manuscript Author Manuscript Author Manuscript Author Manuscript

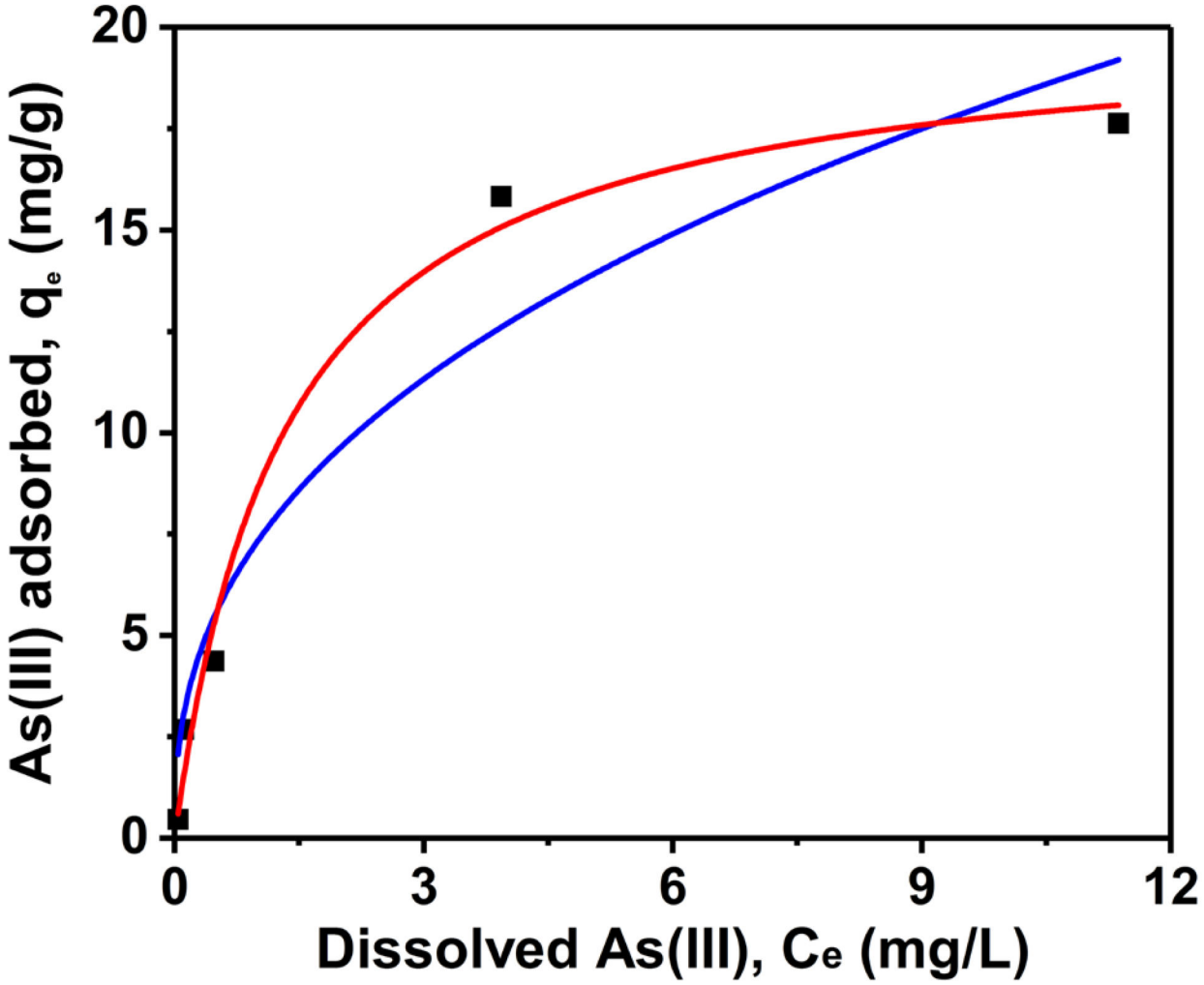

Fig. 3.

Adsorption isotherms of As(III) on CeO_2 NPs in the bioassay medium (MEM). The square markers are the experimental data; the red and blue lines are the Langmuir and Freundlich fitting.

Author Manuscript Author Manuscript Author Manuscript Author Manuscript

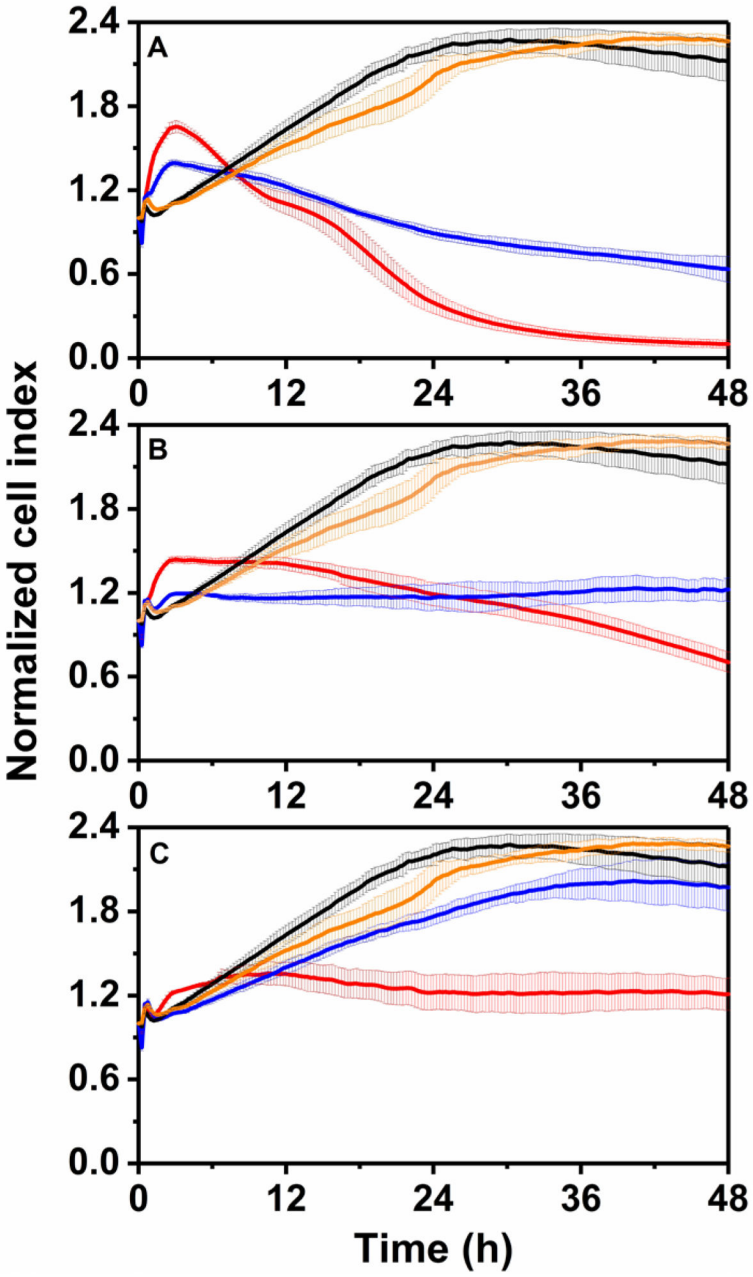

Fig. 4.

Dynamic cytotoxicity response of 16HBE14o- human bronchial epithelial cells exposed to different concentrations of As(III) in the presence and absence of CeO_2 NPs. As(III) concentrations: 5.0 mg/L (panel A), 2.5 mg/L (panel B) and 0.5 mg/L (panel C). The black lines represent the NP and As(III) free control; the yellow lines are the samples only exposed to 250 mg/L CeO_2 NPs; the red lines show the samples treated with As(III) alone; the blue lines are the samples exposed to As(III) solutions adsorbed to CeO_2 NPs.

Author Manuscript Author Manuscript Author Manuscript Author Manuscript

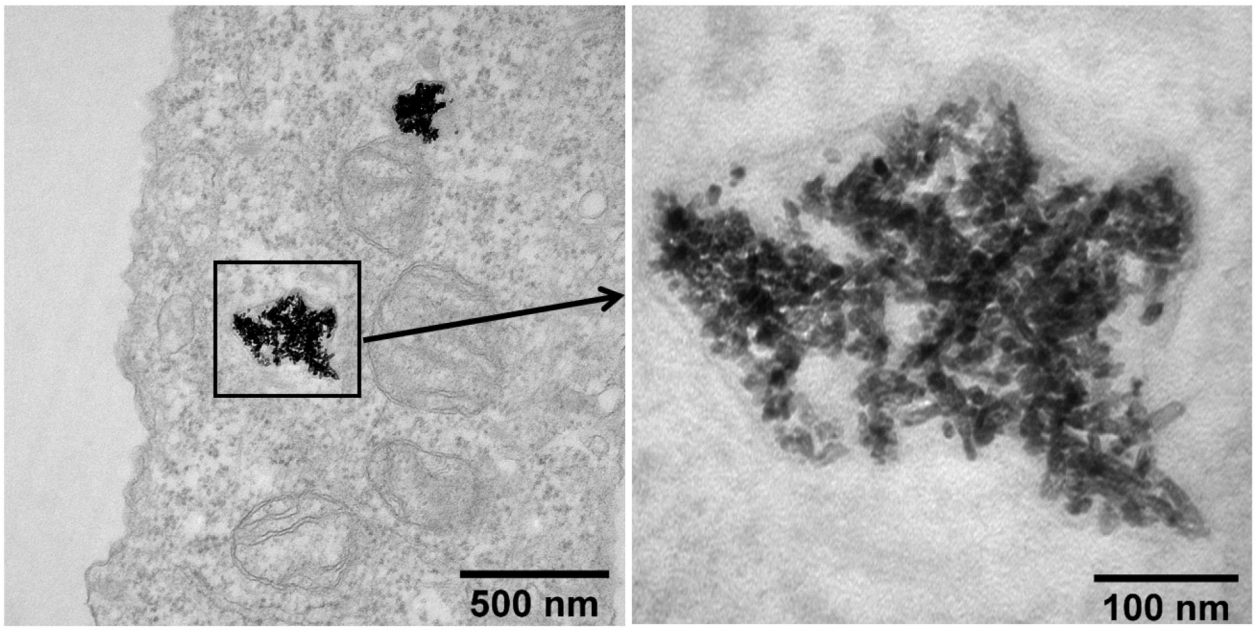

Fig. 5.
TEM image of CeO_2 NPs in 16HBE14o- human bronchial epithelial cells.

Author Manuscript

Author Manuscript

Author Manuscript

Author Manuscript

Table 1

Equilibrium adsorption isotherm fitting parameters for As(III) onto CeO_2 NPs in MEM.

Model	**Langmuir**			**Freundlich**		
Parameters	q_{max} [mg/g]	K_{eq} [L/mg]	R^2	K_f [(mg/g)/(mg/L)$^{1/n}$]	n	R^2
	20.21	0.75	0.98	7.32	2.52	0.91

Author Manuscript

Author Manuscript

Author Manuscript

Author Manuscript

Table 2

Concentrations of dissolved As after 2-day pre-adsorption in the presence and absence of CeO_2 NPs (250 mg/L).

Sample Composition	As Concentration (mg/L)
5.0 mg/L of As(III)	4.93
5.0 mg/L of As(III) with CeO_2 NP	1.36
2.5 mg/L of As(III)	2.47
2.5 mg/L of As(III) with CeO_2 NP	0.29
0.5 mg/L of As(III)	0.50
0.5 mg/L of As(III) with CeO_2 NP	0.03